Received 8 June 2023; revised 30 August 2023; accepted 2 October 2023. Date of publication 6 October 2023; date of current version 19 December 2023. Recommended by Senior Editor Prof. Wei Zhang.

Digital Object Identifier 10.1109/OJCSYS.2023.3322636

Adaptive Control for Singularly Perturbed Systems

KAMERON EVES [1] (Member, IEEE), AND JOHN VALASEK [2] (Senior Member, IEEE)

[1]Utah Tech University, St. George, UT 84770 USA
[2]Texas A&M University, College Station, TX 77843-3141 USA

CORRESPONDING AUTHOR: KAMERON EVES (e-mail: kameron.eves@utahtech.edu).

This work was supported by the U.S. Navy Office of Naval Research under Contract N00014-23-1-2412.

ABSTRACT Singularly perturbed systems are a class of mathematical systems that are not well approximated by their limits and can be used to model plants with multiple fast and slow states. Multiple-timescale systems are very common in engineering applications, but adaptive control can be sensitive to timescale effects. Recently a method called [K]control of Adaptive Multiple-timescale Systems (KAMS) has shown improved performance and increased robustness for singularly perturbed systems, but it has only been studied on systems using adaptive control for the slow states. This article extends KAMS to the general case when adaptive control is used to stabilize both the slow and fast states simultaneously. This causes complex interactions between the fast state reference model and the manifold to which the fast states converge. It is proven that under certain conditions the system still converges to the reference model despite these complex interactions. This method is demonstrated on a nonlinear, nonstandard, numerical example.

INDEX TERMS Adaptive control, nonlinear systems and control, perturbation techniques, timescales.

I. INTRODUCTION

Singularly perturbed differential equations can be used to model systems with elements that evolve at different rates. For example, singularly perturbed models have been published for aircraft [1], spacecraft [1], electric motors [2], nuclear reactors [2], factory logistics [3], and pandemics [4]. Whereas adaptive controllers have sometimes been developed for the systems listed above, these adaptive methods have largely ignored the timescale separation (termed Full-Order Adaptive Control (FOAC)) or used sequential loop closure (e.g. [5], [6]). Singular perturbation theory is a more precise method of dealing with timescale behavior, but adaptive control research to date in the literature lacks a rigorous analytical method to check for stability in the presence of singularly perturbed plants.

Singular perturbation theory is a broad mathematical field that has been used in adaptive control *design* [7], [8], [9], but relatively little research addresses *plants* that are modeled with singularly perturbed differential equations. Researchers who have used adaptive control on singularly perturbed plants have primarily applied their methods to only a subset of the states and ignored the other dynamics [4], [10], [11]. This method is called Reduced-Order Adaptive Control (ROAC) and it fails when the ignored dynamics are unstable [12].

Multiple-timescale control is a branch of control theory that specifically addresses singularly perturbed plants. However, adaptive control has yet to be considered by multiple-timescale control researchers. Saha and Valasek designed controllers for uncertain singularly perturbed plants [13], [14], [15], [16], but their method derives the adaption laws using a full-order Lyapunov analysis. This makes their method difficult to generalize.

This article extends the [K]control of Adaptive Multiple-timescale Systems (KAMS) methodology which was first introduced and developed in [12]. KAMS provides a flexible framework that enables a wide class of modern adaptive methods to be applied to singularly perturbed systems. Compared to FOAC, ROAC, and sequential loop closure KAMS is more robust and rigorous. Compared to Saha and Valasek's method, KAMS is more general.

The singularly perturbed nature of the plant causes a subset of the states to evolve significantly faster than the other states. The general premise of KAMS is to use geometric singular perturbation theory to fully decouple the fast and slow states [17]. Two different adaptive controllers can then be designed in isolation for these two independent subsystems. The independent control signals are fused using a wide class of methods from the field of multiple-timescale control. These multiple-timescale control fusion techniques have not been studied in the presence of adaptive control. KAMS addresses this gap in the literature.

Allowing adaptive control in both the fast and slow states is a challenging problem because of complex interactions between the slow timescale trajectory of the fast states and the fast state reference model. The present work builds upon the author's prior work [12] which discusses the much simpler case of adaptive control for only the slow states. Unlike [12], the present work makes no prior assumptions about the stability of the plant subsystems. The novel contribution of the present work is formal proof that under certain conditions the coupling present in the more accurate full-order model is insufficient to destabilize these adaptive controllers even though they are designed in isolation.

Section II details the KAMS control framework and associated singular perturbation analysis that is used to decouple the subsystems. In Section III, a set of conditions are derived that are sufficient to show that the states converge to their reference models. Finally, in Section IV an example of KAMS on a nonlinear nonstandard system is given. This example demonstrates how methods common in the literature - Sequential Control and Adaptive Nonlinear Dynamic Inversion (ANDI) - can be used on singularly perturbed systems within the framework of KAMS.

II. CONTROL SYNTHESIS

This section introduces KAMS, explains the assumptions, and describes the notation. For more details, the reader is referred to [18], [19], [20] for adaptive control, [17], [21] for multiple-timescale control, [22] for singular perturbation theory, and [23] for differential geometry in the context of control theory.

A. SYSTEM DESCRIPTION

This work addresses singularly perturbed systems that model multiple-timescale plants. A *singularly perturbed system* is a system that is a function of a small scalar ϵ but not well approximated by the limit as that scalar approaches zero. This scalar is called the singular perturbation parameter. The *timescale* of a system is a measure of how quickly a system's states evolve. The systems considered in this article have two timescales. The slow states ($\boldsymbol{x} \in \mathbb{D}_x^{n_x} \subseteq \mathbb{R}^{n_x}$) evolve on the slow timescale (t_s) and the fast states ($\boldsymbol{z} \in \mathbb{D}_z^{n_z} \subseteq \mathbb{R}^{n_z}$) evolve on the fast timescale (t_f). Conversion between fast time and slow time is a change of units. Let the timescale separation parameter be the ratio of the two timescales $\epsilon \triangleq t_s/t_f$. It can be shown that $0 < \epsilon \ll 1$. The derivative with respect to the fast timescale is denoted $d(\cdot)/dt_f \triangleq (\grave{\cdot})$ and the derivative with respect to the slow timescale is denoted $d(\cdot)/dt_s \triangleq (\acute{\cdot})$. Using the above definitions it can be shown that $(\grave{\cdot}) = \epsilon(\acute{\cdot})$. As a general rule $\acute{z} \gg \acute{x}$ and $\epsilon\acute{z} \approx \acute{x}$. Whereas these relationships are not always true, they provide good intuition behind the meaning of the timescale separation parameter. Multiple-timescale plants can be modeled using singular perturbation theory by making the timescale separation parameter a singular perturbation parameter.

This work is generalized to the class of systems which are uncertain, nonlinear, multiple-input multiple-output (MIMO) plants of the form

$$\acute{\boldsymbol{x}} = f_x(\boldsymbol{x}, \boldsymbol{z}, \boldsymbol{u}) \tag{1a}$$

$$\epsilon\acute{\boldsymbol{z}} = f_z(\boldsymbol{x}, \boldsymbol{z}, \boldsymbol{u}, \epsilon) \tag{1b}$$

where $\boldsymbol{u} \in \mathbb{R}^{n_u}$ is the system input. This system is singularly perturbed because because $0 < \epsilon \ll 1$ and the functions f_x and f_z are defined such that $\mathcal{O}(f_x) = \mathcal{O}(f_z) = \mathcal{O}(1)$. The order of a function (i.e. the output of the $\mathcal{O}$ operator) is a measure of the rate of change of that function as $\epsilon \to 0$. See [17, Appendix A.2] for a more formal definition.

Remark 1: Single-timescale systems can be written in the format described by (1). However, applying a multiple-timescale control technique to a single timescale system comes with a performance penalty. The resulting closed-loop responses will be slower. This effect was identified and explored in [24] and [25]. Oliveira et al. demonstrated this effect on during a neuromuscular electrical stimulation experiment [26].

B. SINGULAR PERTURBATION ANALYSIS

Geometric singular perturbation theory shows that the system can be approximated by two different asymptotic solutions. The first system is found by taking the limit as $\epsilon \to 0$

$$\acute{\boldsymbol{x}} = f_x(\boldsymbol{x}, \boldsymbol{z}_s, \boldsymbol{u}) \tag{2a}$$

$$0 = f_z(\boldsymbol{x}, \boldsymbol{z}_s, \boldsymbol{u}, 0) \tag{2b}$$

and is called the *reduced slow subsystem*. It is only a valid approximation when $t \gg 0$. Note that the fast states are constrained to a subset of their domain $\boldsymbol{z}_s \in \mathbb{D}_{z_s}^{n_z} \subseteq \mathbb{D}_z^{n_z}$ where $\boldsymbol{z}_s$ is the root of (2b). In multiple-timescale control, $\boldsymbol{z}_s$ is called the *manifold*. If (2b) can be solved for $\boldsymbol{z}_s$ then the system is called *standard*. The second asymptotic solution for (1) is found by performing a change of timescales (recall that $(\grave{\cdot}) = \epsilon(\acute{\cdot})$) and again taking the limit as $\epsilon \to 0$

$$\grave{\boldsymbol{x}} = 0 \tag{3a}$$

$$\grave{\boldsymbol{z}} = f_z(\boldsymbol{x}, \boldsymbol{z}, \boldsymbol{u}, 0) \tag{3b}$$

This is called the *reduced fast subsystem* and is only a valid approximation when t is very close to 0.

C. ADAPTIVE CONTROL

The control objective of this work is to determine the input as a function of the states that permits the full-order system to track a reference model asymptotically. The first step in this process is to design two different adaptive control algorithms that stabilize the reduced subsystems individually. Many adaptive control algorithms are available in the literature for this purpose. This article addresses a wide class of algorithms that fit the format described in this section. The input to the slow subsystem is $\boldsymbol{u}_s \in \mathbb{R}^{n_u}$ and the input to the fast subsystems is $\boldsymbol{u}_f \in \mathbb{R}^{n_u}$. The variables $\boldsymbol{x}_m \in \mathbb{D}_x^{n_x}$ and $\boldsymbol{z}_m \in \mathbb{D}_z^{n_z}$ are reference model states. The parameters $\hat{\boldsymbol{\theta}}_x \in \mathbb{P}_{\theta_x}^{n_{\theta x}} \subseteq \mathbb{R}^{n_{\theta_x}}$ and $\hat{\boldsymbol{\theta}}_z \in \mathbb{P}_{\theta_z}^{n_{\theta z}} \subseteq \mathbb{R}^{n_{\theta_z}}$ are adaptive estimates of the true parameters $\boldsymbol{\theta}_x$ and $\boldsymbol{\theta}_z$ respectively. The true parameters are allowed to be time-varying. Let

$$\boldsymbol{\theta}_x = g_{\theta_x}(t_s) \quad (4a)$$

$$\boldsymbol{\theta}_z = g_{\theta_z}(t_f) \quad (4b)$$

$$\acute{\boldsymbol{\theta}}_x = f_{\theta_x}(t_s) \quad (4c)$$

$$\grave{\boldsymbol{\theta}}_z = f_{\theta_z}(t_f) \quad (4d)$$

Define $\boldsymbol{r}_x \in \mathbb{R}^{n_{r_x}}$ to be the bounded input to the slow state reference model and a function of time. This function and its derivative are

$$\boldsymbol{r}_x = g_{r_x}(t_s) \quad (5a)$$

$$\acute{\boldsymbol{r}}_x = f_{r_x}(t_s) \quad (5b)$$

The reference models and adaptation laws must be selected in tandem with the control input so that the control objective is achieved. The differential equations describing the evolution of the reference models and parameter estimates are of the form

$$\acute{\boldsymbol{x}}_m = f_{x_m}(\boldsymbol{x}, \boldsymbol{x}_m, \hat{\boldsymbol{\theta}}_x, t_s) \quad (6a)$$

$$\acute{\hat{\boldsymbol{\theta}}}_x = f_{\hat{\theta}_x}(\boldsymbol{x}, \boldsymbol{x}_m, \hat{\boldsymbol{\theta}}_x, t_s) \quad (6b)$$

$$\grave{z}_m = f_{z_m}(\boldsymbol{x}, \boldsymbol{x}_m, \hat{\boldsymbol{\theta}}_x, z, z_m, \hat{\boldsymbol{\theta}}_z, t_f) \quad (6c)$$

$$\grave{\hat{\boldsymbol{\theta}}}_z = f_{\hat{\theta}_z}(\boldsymbol{x}, \boldsymbol{x}_m, \hat{\boldsymbol{\theta}}_x, z, z_m, \hat{\boldsymbol{\theta}}_z, t_f) \quad (6d)$$

Remark 2: Note that $\boldsymbol{r}_x$ is implicitly included as a possible input to these functions because it is fully described by time. A wide array of adaptive methods fit this format (e.g. [18], [27]).

The role of the timescale separation parameter is important in these equations. If the control input is incorrectly designed then the timescale analysis in the previous section could be invalidated. The following two assumptions are made to prevent that.

Assumption 1: The manifold is an asymptotically stable equilibrium of the fast reference model in the reduced fast subsystem.

Assumption 2: The timescale of the reference models, the slow state reference model input, and the adaptation laws all match the timescale of the subsystem to which they are applied. Mathematically this means that $\mathcal{O}(f_{x_m}) = \mathcal{O}(f_{\hat{\theta}_x}) = \mathcal{O}(f_{\theta_x}) = \mathcal{O}(f_{z_m}) = \mathcal{O}(f_{\hat{\theta}_z}) = \mathcal{O}(f_{\theta_z}) = \mathcal{O}(f_{r_x}) = \mathcal{O}(1)$

These assumptions are intuitive. For example, if the reference model for the slow states evolved on the fast timescale then the slow states would not be able to keep up - or, more precisely, their evolution could not be decoupled from the fast states.

D. MULTIPLE-TIMESCALE FUSION

The inputs to the reduced-order subsystems have been defined and will form the building blocks of the full-order system input. Let the full-order input take the form

$$\boldsymbol{u} = g_u(\boldsymbol{x}, \boldsymbol{x}_m, \hat{\boldsymbol{\theta}}_x, z, z_m, \hat{\boldsymbol{\theta}}_z, t_s) \quad (7)$$

The stability analysis in the next section depends upon the reduced-order models being stabilized by their inputs $\boldsymbol{u}_s$ and $\boldsymbol{u}_f$. The control objective is to select $\boldsymbol{u}$ so that a singular perturbation analysis reduces $\boldsymbol{u}$ to $\boldsymbol{u}_s$ and $\boldsymbol{u}_f$. Thus the reduced-order systems are simultaneously stabilized by a single input $\boldsymbol{u}$. Various multiple-timescale control techniques accomplish this objective by fusing the control signals for the two reduced subsystems. Three candidate methods are summarized. See [17] for more information on each of these methods.

1) COMPOSITE CONTROL

Composite Control [21, p. 94-102] selects the control input to be $\boldsymbol{u} = \boldsymbol{u}_s + \boldsymbol{u}_f$ where $\boldsymbol{u}_f = 0$ when $z = z_s$. The engineer first selects $\boldsymbol{u}_s$ so that the reduced slow model is stable. Then the engineer selects $\boldsymbol{u}_f$ so that $\boldsymbol{u}_s + \boldsymbol{u}_f$ drives the fast states to $z = z_s$. This requires prior knowledge of the system's open-loop manifold so the system must be of standard form. Composite Control (non-adapting) has seen many industrial applications including flexible robotics [28], electrical circuits [29], and chemical reactions [30].

2) SEQUENTIAL CONTROL

In Sequential Control [17] the fast states are used as the input to the slow subsystem. The manifold is selected such that the slow states converge to their reference model by setting $z_s = \boldsymbol{u}_s$ Then the input $\boldsymbol{u}$ can be selected to drive the fast states to the manifold. Thus Sequential Control uses $\boldsymbol{u} = \boldsymbol{u}_f$. Valasek, Narang-Siddarth, and Saha applied Sequential Control (non-adapting) to two-core coupled nuclear reactor stabilization [17, p. 122-127] and a nonlinear spring spring-mass-damper [31], [32].

3) SIMULTANEOUS SLOW AND FAST TRACKING

Simultaneous Slow and Fast Tracking [2] uses the input $\boldsymbol{u} = \boldsymbol{u}_s = \boldsymbol{u}_f$ to stabilize both reduced-order systems simultaneously. As such this method is not suitable for underactuated systems. The advantage of this method is that the slow states and the fast states can both be commanded to any arbitrary trajectory within the state space (constrained only by timescales and smoothness). Unlike Composite Control and Sequential Control, Simultaneous Slow and Fast Tracking allows an arbitrary manifold. Narang-Siddarth and Valasek used Simultaneous Slow and Fast Tracking (non-adapting) to control an F/A-18 A Hornet through an aggressive vertical climb and roll maneuver [2].

A block diagram for the KAMS control framework described in the previous section is given in Fig. 1. As defined in the previous section the fast adaptive control is allowed to be

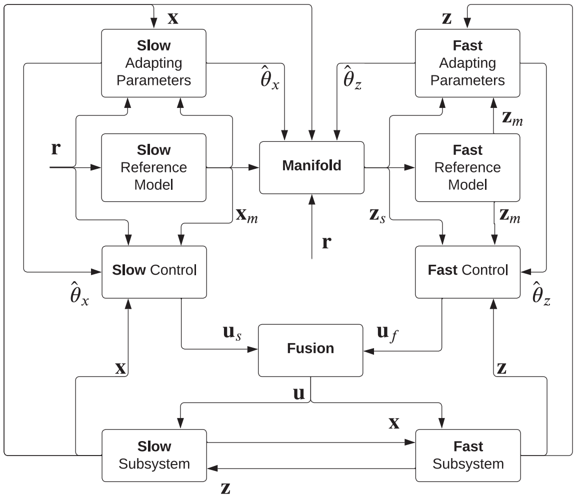

FIGURE 1. **A block diagram of KAMS.**

a function of the slow states. This uncommon case is excluded from the block diagram for readability.

III. STABILITY ANALYSIS

This section develops tools for stability analysis of the full-order system. Whereas the adaptive controllers have been designed so that the reduced-order systems are well-behaved, these properties might not extend to the coupled full-order system. The system of equations is rewritten as a single augmented system in terms of the error coordinates for notational simplicity. Examining the differential geometric nature of the augmented system leads to the desired important insights into the behavior of the full-order system.

A. AUGMENTED ERROR DYNAMICS

Adaptive control adds additional states (i.e. the reference model and adapting parameters) to the closed-loop system. These states evolve (see (6)) and effectively create a coupled augmented closed-loop system with control states and system states. The augmented closed-loop system is defined in this section.

The variables which describe the state of the system are $\boldsymbol{x}$, $\boldsymbol{x}_m$, $\hat{\boldsymbol{\theta}}_x$, z, z_m, and $\hat{\boldsymbol{\theta}}_z$. For notational simplicity, these states are concatenated together. Define

$$\boldsymbol{\xi} \triangleq \begin{bmatrix} \boldsymbol{x}^T & \boldsymbol{x}_m^T & \hat{\boldsymbol{\theta}}_x^T \end{bmatrix}^T \quad \in \mathbb{D}_\xi^{n_\xi} \tag{8a}$$

$$\boldsymbol{\eta} \triangleq \begin{bmatrix} z^T & z_m^T & \hat{\boldsymbol{\theta}}_z^T \end{bmatrix}^T \quad \in \mathbb{D}_\eta^{n_\eta} \tag{8b}$$

$$\boldsymbol{\phi} \triangleq \begin{bmatrix} \boldsymbol{\xi}^T & \boldsymbol{\eta}^T \end{bmatrix}^T \quad \in \mathbb{D}_\phi^{n_\phi} \tag{8c}$$

Note that the differential equations describing the evolution of $\boldsymbol{\phi}$ are found in (1) and (6) are dependent upon the system state variables, the input, and time. However, the input is also a function of the system state variables and time (see (7)) so the system's dynamics are entirely described by the system's state and time. Similarly, the manifold is a function of the slow states and the input (see (2b)) so it too can be described by a function of the system state and time. Let that function and its time derivative be

$$z_s = g_{z_s}(\boldsymbol{x}, \boldsymbol{x}_m, \hat{\boldsymbol{\theta}}_x, \hat{\boldsymbol{\theta}}_z, t_s) \tag{9a}$$

$$\acute{z}_s = f_{z_s}(\boldsymbol{x}, \boldsymbol{x}_m, \hat{\boldsymbol{\theta}}_x, z, z_m, \hat{\boldsymbol{\theta}}_z, t_s) \tag{9b}$$

The following assumption is made:

Assumption 3: g_{z_s} is a diffeomorphism and the manifold evolves in the slow timescale so $\mathcal{O}(f_{z_s}) = \mathcal{O}(1)$.

Section III-C discusses the manifold in more detail.

If the control objective for the full-order system is successfully achieved then two things occur as $\boldsymbol{t} \to \infty$. First $z \to z_m \to z_s$. This is followed by $\boldsymbol{x} \to \boldsymbol{x}_m$. These goals imply a set of error variables. Define

$$\boldsymbol{e}_x \triangleq \boldsymbol{x} - \boldsymbol{x}_m \quad \in \mathbb{B}^{n_x}(r_{e_\phi}) \tag{10a}$$

$$\tilde{\boldsymbol{x}}_m \triangleq \boldsymbol{x}_m - \boldsymbol{r}_x \quad \in \mathbb{B}^{n_x}(r_{e_\phi}) \tag{10b}$$

$$\tilde{\boldsymbol{\theta}}_x \triangleq \hat{\boldsymbol{\theta}}_x - \boldsymbol{\theta}_x \quad \in \mathbb{B}^{n_{\theta_x}}(r_{e_\phi}) \tag{10c}$$

$$\tilde{z} \triangleq z - z_s \quad \in \mathbb{B}^{n_z}(2r_{e_\phi}) \tag{10d}$$

$$\tilde{z}_m \triangleq z_m - z_s \quad \in \mathbb{B}^{n_z}(r_{e_\phi}) \tag{10e}$$

$$\boldsymbol{e}_z \triangleq z - z_m \quad \in \mathbb{B}^{n_z}(r_{e_\phi}) \tag{10f}$$

$$\tilde{\boldsymbol{\theta}}_z \triangleq \hat{\boldsymbol{\theta}}_z - \boldsymbol{\theta}_z \quad \in \mathbb{B}^{n_{\theta_z}}(r_{e_\phi}) \tag{10g}$$

where $r_{e_\phi} \in \mathbb{R}_+$. Whereas $\boldsymbol{x}_m$, $\hat{\boldsymbol{\theta}}_x$, and $\hat{\boldsymbol{\theta}}_z$ don't necessarily converge to $\boldsymbol{r}_x$, $\boldsymbol{\theta}_x$, and $\boldsymbol{\theta}_z$ respectively their relationship is nonetheless important. Note that

$$\boldsymbol{e}_z = \tilde{z} - \tilde{z}_m \tag{11}$$

A change of variables is now performed to describe the system in terms of the error variables. The new system state variables are

$$\boldsymbol{e}_\xi \triangleq \begin{bmatrix} \boldsymbol{e}_x^T & \tilde{\boldsymbol{x}}_m^T & \tilde{\boldsymbol{\theta}}_x^T \end{bmatrix}^T \quad \in \mathbb{B}^{n_\xi}(r_{e_\phi}) \tag{12a}$$

$$\boldsymbol{e}_\eta \triangleq \begin{bmatrix} \boldsymbol{e}_z^T & \tilde{z}_m^T & \tilde{\boldsymbol{\theta}}_z^T \end{bmatrix}^T \quad \in \mathbb{B}^{n_\eta}(r_{e_\phi}) \tag{12b}$$

$$\boldsymbol{e}_\phi \triangleq \begin{bmatrix} \boldsymbol{e}_\xi^T & \boldsymbol{e}_\eta^T \end{bmatrix}^T \quad \in \mathbb{B}^{n_\phi}(r_{e_\phi}) \tag{12c}$$

Let the mapping $h : \mathbb{B}^{n_\phi}(r_{e_\phi}) \times \mathbb{R}_+ \to \mathbb{D}_\phi^{n_\phi} \times \mathbb{R}_+$ be the diffeomorphism between the two sets of state variables

$$(\boldsymbol{\phi}, t_s) = h(\boldsymbol{e}_\phi, t_s) \tag{13}$$

where $\boldsymbol{\phi}$ is

$$\boldsymbol{\phi} = \begin{bmatrix} \boldsymbol{e}_x + \tilde{\boldsymbol{x}}_m + g_{r_x}(t_s) \\ \tilde{\boldsymbol{x}}_m + g_{r_x}(t_s) \\ \tilde{\boldsymbol{\theta}}_x + g_{\theta_x}(t_s) \\ \boldsymbol{e}_z + \tilde{z}_m + g_{z_s}(\cdot) \\ \tilde{z}_m + g_{z_s}(\cdot) \\ \tilde{\boldsymbol{\theta}}_z + g_{\theta_z}(t_s/\epsilon) \end{bmatrix} \tag{14}$$

and

$$g_{z_s}(\cdot) = g_{z_s}(\boldsymbol{e}_x + \tilde{\boldsymbol{x}}_m + g_{r_x}(t_s), \quad \tilde{\boldsymbol{x}}_m + g_{r_x}(t_s), \quad \tilde{\boldsymbol{\theta}}_x + g_{\theta_x}(t_s), \quad \tilde{\boldsymbol{\theta}}_z + g_{\theta_z}(t_s/\epsilon), \quad t_s) \tag{15}$$

Equations (1) and (6) can be rewritten in terms of the new state variables as

$$\acute{\boldsymbol{e}}_x = f_x \circ h(\boldsymbol{e}_\xi, \boldsymbol{e}_\eta, t_s) - f_{x_m} \circ h(\boldsymbol{e}_\xi, t_s) \quad (16a)$$

$$\acute{\tilde{\boldsymbol{x}}}_m = f_{x_m} \circ h(\boldsymbol{e}_\xi, t_s) - f_{r_x}(t_s) \quad (16b)$$

$$\acute{\tilde{\boldsymbol{\theta}}}_x = f_{\hat{\theta}_x} \circ h(\boldsymbol{e}_\xi, t_s) - f_{\theta_x}(t_s) \quad (16c)$$

$$\epsilon\acute{\boldsymbol{e}}_z = f_z \circ h(\boldsymbol{e}_\xi, \boldsymbol{e}_\eta, t_s, \epsilon) - f_{z_m} \circ h(\boldsymbol{e}_\xi, \boldsymbol{e}_\eta, t_s) \quad (16d)$$

$$\epsilon\acute{\tilde{\boldsymbol{z}}}_m = f_{z_m} \circ h(\boldsymbol{e}_\xi, \boldsymbol{e}_\eta, t_s) - \epsilon f_{z_s} \circ h(\boldsymbol{e}_\xi, \boldsymbol{e}_\eta, t_s) \quad (16e)$$

$$\epsilon\acute{\tilde{\boldsymbol{\theta}}}_z = f_{\hat{\theta}_z} \circ h(\boldsymbol{e}_\xi, \boldsymbol{e}_\eta, t_s) - f_{\theta_z}(t_f) \quad (16f)$$

This system can be written simply as

$$\acute{\boldsymbol{e}}_\xi = f_{e_\xi}(\boldsymbol{e}_\xi, \boldsymbol{e}_\eta, t_s) \quad (17a)$$

$$\epsilon\acute{\boldsymbol{e}}_\eta = f_{e_\eta}(\boldsymbol{e}_\xi, \boldsymbol{e}_\eta, t_s, \epsilon) \quad (17b)$$

or even simpler as

$$\acute{\boldsymbol{e}}_\phi = f_{e_\phi}(\boldsymbol{e}_\phi, t_s, \epsilon) \quad (18)$$

where f_{e_ξ}, f_{e_η}, and f_{e_ϕ} are defined such that (17) and (18) are identically equal to the vector field in (16). This last representation obscures the timescale behavior because $\mathcal{O}(f_{e_\phi}) \neq \mathcal{O}(1)$. Equation (17) is recognizable as a singularly perturbed system of the type typically studied by multiple-timescale control researchers. In fact, traditional analysis tools are applicable. However, because the form of (16) is available additional insights are available.

Let the subscript s be used to denote a variable or vector field on the slow subsystem manifold, e.g. $\boldsymbol{e}_{\eta,s}$ represents $\boldsymbol{e}_\eta$ when $z = z_m = z_s$. Similarly, let the subscript f represent a variable or vector field on the fast subsystem manifold. The augmented reduced slow subsystem in error coordinates can be found by setting $\epsilon = 0$ and $z = z_m = z_s$ such that

$$\acute{\boldsymbol{e}}_x = f_x \circ h(\boldsymbol{e}_\xi, \boldsymbol{e}_{\eta,s}, t_s) - f_{x_m} \circ h(\boldsymbol{e}_\xi, t_s) \quad (19a)$$

$$\acute{\tilde{\boldsymbol{x}}}_m = f_{x_m} \circ h(\boldsymbol{e}_\xi, t_s) - f_{r_x}(t_s) \quad (19b)$$

$$\acute{\tilde{\boldsymbol{\theta}}}_x = f_{\hat{\theta}_x} \circ h(\boldsymbol{e}_\xi, t_s) - f_{\theta_x}(t_s) \quad (19c)$$

This reduced slow subsystem can be written simply as

$$\acute{\boldsymbol{e}}_\xi = f_{e_\xi,s}(\boldsymbol{e}_\xi, \boldsymbol{e}_{\eta,s}, t_s) \quad (20)$$

where $f_{e_\xi,s}$ is defined such that (20) is identically equal to the vector field in (19). Equation (20) looks very similar to (17) and (18) but represents a fundamentally different vector field which is only defined on a subset of the full-order domain (i.e. where $z = z_m = z_s$). The augmented reduced fast subsystem in error coordinates is

$$\grave{\boldsymbol{e}}_x = 0 \quad (21a)$$

$$\grave{\tilde{\boldsymbol{x}}}_m = 0 \quad (21b)$$

$$\grave{\tilde{\boldsymbol{\theta}}}_x = 0 \quad (21c)$$

$$\grave{\boldsymbol{e}}_z = f_z \circ h(\boldsymbol{e}_\xi, \boldsymbol{e}_\eta, t_s, 0) - f_{z_m} \circ h(\boldsymbol{e}_\xi, \boldsymbol{e}_\eta, t_s) \quad (21d)$$

$$\grave{\tilde{\boldsymbol{z}}}_m = f_{z_m} \circ h(\boldsymbol{e}_\xi, \boldsymbol{e}_\eta, t_s) - 0 \quad (21e)$$

$$\grave{\tilde{\boldsymbol{\theta}}}_z = f_{\hat{\theta}_z} \circ h(\boldsymbol{e}_\xi, \boldsymbol{e}_\eta, t_s) - f_{\theta_z}(t_f) \quad (21f)$$

This reduced fast subsystem can be written simply as

$$\grave{\boldsymbol{e}}_\xi = f_{e_\xi,f}(\boldsymbol{e}_\xi, \boldsymbol{e}_\eta, t_f) \quad (22a)$$

$$\grave{\boldsymbol{e}}_\eta = f_{e_\eta,f}(\boldsymbol{e}_\xi, \boldsymbol{e}_\eta, t_f) \quad (22b)$$

or even simpler as

$$\acute{\boldsymbol{e}}_\phi = f_{e_\phi,f}(\boldsymbol{e}_\phi, t_f) \quad (23)$$

where $f_{e_\xi,f}$, $f_{e_\eta,f}$, and $f_{e_\phi,f}$ are defined such that (22) and (23) are identitically equal to the vector field in (21). Finally, in the reduced fast subsystem

$$\grave{\boldsymbol{r}}_x = 0 \quad (24a)$$

$$\grave{\boldsymbol{\theta}}_x = 0 \quad (24b)$$

$$\grave{z}_s = 0 \quad (24c)$$

by Assumptions 2 and 3.

B. DIFFERENTIAL GEOMETRY

Differential geometry is a natural fit for the analysis of singularly perturbed systems because the differential equations which describe these systems form nonautonomous vector fields on a topological manifold. The term *manifold* has been used somewhat informally and will continue to be used to refer to z_s. But it is worth noting that the reduced subsystems form differential submanifolds embedded within the full-order system manifold in the topological sense. Thus it is clear that g_s is a diffeomorphic chart between the full-order manifold ($\mathcal{M}$) and the reduced slow manifold ($\mathcal{M}_s$). The chart between the full-order manifold and the reduced fast manifold ($\mathcal{M}_f$) is the trivial automorphism. The stability analysis to follow will involve the time derivative of Lyapunov functions along a vector field that is a subset of the tangent bundle of one of these topological manifolds. The notation $\mathcal{L}(\cdot)$ is used to represent the Lie derivative along the vector field given in the parentheses (the traditional subscript notation is not used to ensure the subscripts on the functions are readable). Let $|(\cdot)|_p$ be the l_p norm of a vector or the induced l_p norm of a matrix and let $\|(\cdot)\|_p$ be the L_p norm over time where $p \in [1, \infty]$. If the L_p norm is applied to a vector then it means the L_p norm of each component of the vector. Unless otherwise specified, all sets are subsets of the Euclidean Hilbert space with the dimension given in the superscript. An integer subscript $(\cdot)_i$ on a variable (not to be confused with the subscript on the p-norms) represents the ith element of the vector.

C. MANIFOLD AND THE REFERENCE MODEL

The stability proofs in the next section are significantly complicated by the relationship between the manifold and the fast reference model. Traditional multiple-timescale control and adaptive control both use a feedback loop to ensure closed-loop stability. These feedback loops still exist in the KAMS control architecture. Fig. 2 is the block diagram of KAMS from Fig. 1 except that the traditional feedback loop has been highlighted. All paths which contribute to this loop are bolded but the primary loop is blue. However, KAMS has another unconventional feedback loop because the fast

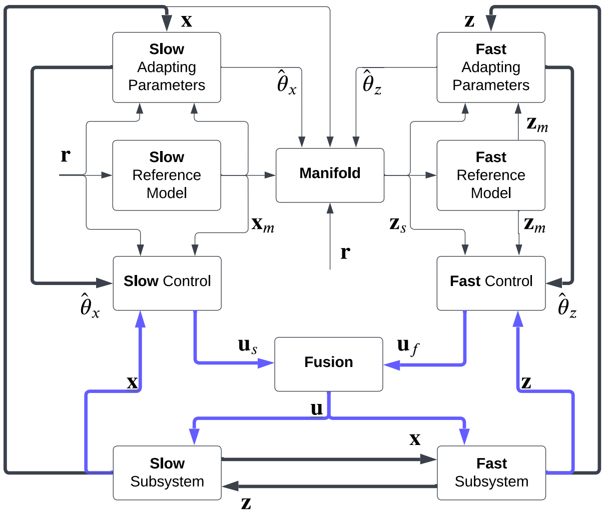

FIGURE 2. The primary feedback loop of KAMS.

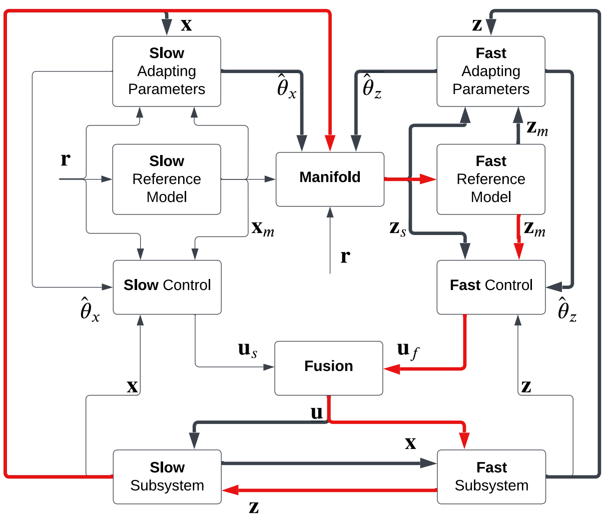

FIGURE 3. The unconventional feedback loop of KAMS.

reference model uses the manifold as an input (Fig. 1), the manifold is a function of the slow states (see (9)), the slow states are coupled with the fast states, and the control objective is for the fast states to track the fast reference model which is itself a function of the manifold. This creates a feedback loop that is typically not seen in adaptive control. Fig. 3 highlights this feedback loop. Again, all paths which contribute to this loop are bolded but the primary unconventional loop is red.

The reference model adds a complication that is not encountered in traditional multiple-timescale control. If the fast reference model is not asymptotically stable then the steady state trajectory for the slow states may not be the manifold. This calls into question the validity of the slow subsystem and means that the multiple-timescale fusion stability proofs in prior work are not applicable. These effects are unavoidable because the full-order stability analysis works by extending the stability of the reduced subsystems to the full-order system. The slow subsystem assumes that the fast states have reached their manifold, so if the stability of the reduced slow subsystem is to have any bearing on the full-order system then the fast reference model must converge to that manifold. This is the purpose of Assumption 1. Reference models are not usually asymptotically stable when their input is time-varying since they are typically Type 1 linear systems. Thus they are only capable of tracking a step input with zero steady-state error. However, closer examination reveals that Assumption 1 is not as restrictive as it appears. Recall that the manifold is assumed to evolve on the slow timescale. Equation (24c) shows that in the fast timescale $\dot{\mathbf{z}}_s = 0$. Thus the manifold is stationary in the reduced fast subsystem, and even a type 1 reference model can be asymptotically stable. Assumption 1 is usually satisfied. However, the full-order system does not benefit from this simplification. The steady-state value of $\tilde{\mathbf{z}}_m$ influences the form and function of the full-order stability proofs in Section III-D. Three cases are studied:

Case 1: *There exist no prior assumptions about the stability of the fast reference model in relation to the full-order manifold.* This is the most general case considered, but also has the most restrictive conditions. This case often requires the control objective to be downgraded to a regulation problem.

Case 2: *The fast reference model is always on the manifold.* This case most commonly occurs when adaptive control is not necessary for the fast subsystem. The fast control drives the fast states directly to the manifold. This type of control can be modeled by setting $\tilde{\mathbf{z}}_m = 0$ and $\dot{\tilde{\boldsymbol{\theta}}}_z = 0$. Note that a parallel simplification exists where there the slow control is non-adaptive, $\tilde{\mathbf{x}}_m = 0$, and $\dot{\tilde{\boldsymbol{\theta}}}_x = 0$ but this still falls within Case 1 above.

Case 3: *The manifold is an asymptotically stable equilibrium of the fast state reference model in the context of the full-order system.* This is possible but requires an unusual reference model. This case is a slightly stricter version of Assumption 1 which only requires asymptotic stability in a subset of the domain.

Remark 3: In the present work, stating that the slow subsystem does not require adaptive control will be equivalent to saying $\tilde{\mathbf{x}}_m = 0$ and $\dot{\tilde{\boldsymbol{\theta}}}_x = 0$. Similarly, stating that the fast subsystem does not require adaptive control will be equivalent to saying $\tilde{\mathbf{z}}_m = 0$ and $\dot{\tilde{\boldsymbol{\theta}}}_z = 0$. This terminology may be slightly misleading because there exist model-free adaptive control algorithms (e.g. [33]) and there exist non-adaptive control methods which require reference models (e.g. Feedback Linearization [34]). However, the intricacies of these methods are not in the scope of this work.

D. FULL-ORDER SYSTEM STABILITY

In this section, the stability of KAMS is analyzed in the context of the full-order system. The goal is to develop conditions that, if met, extend the stability of the reduced subsystems to the full-order system. To that end, four related theorems are proved. Each theorem belongs to one of the three cases described in the previous section. All of the theorems in this work will make use of the vector $\boldsymbol{v} \in \mathbb{R}^4_{\geq 0}$ which is defined as

$$\boldsymbol{v} \triangleq \begin{bmatrix} |\boldsymbol{e}_x|_2 & |\tilde{\boldsymbol{x}}_m|_2 & |\boldsymbol{e}_z|_2 & |\tilde{\boldsymbol{z}}_m|_2 \end{bmatrix}^T \tag{25}$$

1) FOUNDATION OF REDUCED-ORDER STABILITY

The proofs in this section are similar to the proof proposed by [29], [35]. However, they have been significantly altered to account for adaptive control. The general process begins by generating a composite Lyapunov function using Lyapunov functions for the reduced-order subsystems. This composite Lyapunov function is then differentiated along the vector field describing the evolution of the full-order subsystem. Using the stability of the reduced subsystems it is shown that the differences between reduced subsystems and the full-order system are insufficient to violate the negative definiteness. This implies that $\boldsymbol{e}_x, \boldsymbol{e}_z \in L_\infty$ by Lyapunov's direct method [18, Theorem 3.4.1]. The following four Lyapunov functions form the basis of this approach:

$$V_{e_x}(\boldsymbol{e}_x, \tilde{\boldsymbol{\theta}}_x, t_s) : \mathbb{B}^{n_x}(r_{e_\phi}) \times \mathbb{B}^{n_{\theta x}}(r_{e_\phi}) \times \mathbb{R}_+ \to \mathbb{R}_{\geq 0} \tag{26a}$$

$$V_{\tilde{x}_m}(\tilde{\boldsymbol{x}}_m, t_s) : \mathbb{B}^{n_x}(r_{e_\phi}) \times \mathbb{R}_+ \to \mathbb{R}_{\geq 0} \tag{26b}$$

$$V_{e_z}(\boldsymbol{e}_z, \tilde{\boldsymbol{\theta}}_z, t_f) : \mathbb{B}^{n_z}(r_{e_\phi}) \times \mathbb{B}^{n_{\theta z}}(r_{e_\phi}) \times \mathbb{R}_+ \to \mathbb{R}_{\geq 0} \tag{26c}$$

$$V_{\tilde{z}_m}(\tilde{\boldsymbol{z}}_m, t_f) : \mathbb{B}^{n_z}(r_{e_\phi}) \times \mathbb{R}_+ \to \mathbb{R}_{\geq 0} \tag{26d}$$

These Lyapunov functions are positive definite functions of class C^1 (i.e. the function and its derivative are continuous) where $V_{e_x}(0, 0, t_s) = V_{\tilde{x}_m}(0, t_s) = V_{e_z}(0, 0, t_f) = V_{\tilde{z}_m}(0, t_f) = 0$. Let the adaptive control for the reduced subsystems be defined such that

$$\frac{\partial V_{e_x}}{\partial t_s} + \mathcal{L}(f_{e_\xi,s})V_{e_x} \leq -\alpha_1|\boldsymbol{e}_x|_2^2 \tag{27a}$$

$$\frac{\partial V_{e_z}}{\partial t_f} + \mathcal{L}(f_{e_\eta,f})V_{e_z} \leq -\alpha_3|\boldsymbol{e}_z|_2^2 \tag{27b}$$

$$\frac{\partial V_{\tilde{z}_m}}{\partial t_f} + \mathcal{L}(f_{z_m,f})V_{\tilde{z}_m} \leq -\alpha_4|\tilde{\boldsymbol{z}}_m|_2^2 \tag{27c}$$

for some $\alpha_1, \alpha_3, \alpha_4 \in \mathbb{R}_+$. The following assumption is now made:

Assumption 4: The Lyapunov functions V_{e_x}, V_{e_z}, and as needed $V_{\tilde{z}_m}$ are known and exist such that (27) is satisfied.

Note that the existence of $V_{\tilde{z}_m}$ such that (27c) holds is sufficient to guarantee that Assumption 1 is satisfied. After the Lyapunov analysis, Barbalet's Lemma is used to prove convergence [18, Lemma 3.2.5] so the following assumption is made to ensure that the conditions of Barbalet's Lemma are satisfied:

Assumption 5: The functions defined in the present work are sufficiently smooth and bounded so that the function is continuously differentiable as many times as necessary. Sufficiently bounded means that, as necessary, the domain of a function being in L_∞ is sufficient to imply that the function's range is also in L_∞.

The definitions above are a formal way of saying and indeed imply that the adaptive control for the reduced subsystems is well designed. This conclusion only applies to the reduced subsystems.

2) CASE 1

There exist no prior assumptions about the stability of the fast reference model in relation to the full-order manifold.

Theorem 1: Assume $\exists\alpha_2 \in \mathbb{R}_+$, $\exists\beta \in \mathbb{R}_{\geq 0}$, and $\exists\boldsymbol{\gamma}, \boldsymbol{\delta} \in \mathbb{R}^4_{\geq 0}$ such that

$$\frac{\partial V_{\tilde{x}_m}}{\partial t_s} + \mathcal{L}(f_{\tilde{x}_m})V_{\tilde{x}_m} \leq -\alpha_2|\tilde{\boldsymbol{x}}_m|_2^2 \tag{28a}$$

$$\mathcal{L}(f_x - f_{x,s})V_{e_x} \leq \beta|\boldsymbol{e}_x|_2|\tilde{\boldsymbol{z}}|_2 \tag{28b}$$

$$\mathcal{L}(f_z - f_{z,f})V_{e_z} \leq \epsilon\boldsymbol{\gamma}^T\boldsymbol{v}|\boldsymbol{e}_z|_2 \tag{28c}$$

$$-\mathcal{L}(f_{z_s})V_{\tilde{z}_m} \leq \boldsymbol{\delta}^T\boldsymbol{v}|\tilde{\boldsymbol{z}}_m|_2 \tag{28d}$$

Let the matrix $K = K^T$ be defined as

$$K \triangleq \begin{bmatrix} d^*\alpha_1 & 0 & -\frac{1}{2}(d^*\beta + d\gamma_1) & -\frac{1}{2}(d^*\beta + d\delta_1) \\ & d^*\alpha_2 & -\frac{1}{2}d\gamma_2 & -\frac{1}{2}d\delta_2 \\ & & \frac{d}{\epsilon}\alpha_3 - d\gamma_3 & -\frac{1}{2}(d\delta_3 + d\gamma_4) \\ \text{Symmetric} & & & \frac{d}{\epsilon}\alpha_4 - d\delta_4 \end{bmatrix} \tag{29}$$

If $\exists d \in (0, 1)$ and $d^* \triangleq (1 - d)$ such that K is positive definite, then $\boldsymbol{e}_x, \boldsymbol{e}_z \to 0$ as $t \to \infty$.

Proof: Define a composite Lyapunov function

$$V \triangleq d^*(V_{e_x} + V_{\tilde{x}_m}) + d(V_{e_z} + V_{\tilde{z}_m}) \tag{30}$$

Differentiate along the full-order system

$$\acute{V} = d^*\left(\frac{\partial V_{e_x}}{\partial t_s} + \frac{\partial V_{\tilde{x}_m}}{\partial t_s}\right) + d\left(\frac{\partial V_{e_z}}{\partial t_s} + \frac{\partial V_{\tilde{z}_m}}{\partial t_s}\right) \tag{31a}$$

$$+ d^*\mathcal{L}(f_{e_\phi})(V_{e_x} + V_{\tilde{x}_m})d\mathcal{L}(f_{e_\phi})(V_{e_z} + V_{\tilde{z}_m}) \tag{31b}$$

Add and subtract $d^*\mathcal{L}(f_{e_\phi,s})(V_{e_x} + V_{\tilde{x}_m}) + d\mathcal{L}(f_{e_\phi,f})(V_{e_z} + V_{\tilde{z}_m})$

$$\begin{aligned} \acute{V} = {} & d^*\left(\frac{\partial V_{e_x}}{\partial t_s} + \frac{\partial V_{\tilde{x}_m}}{\partial t_s}\right) + d\left(\frac{\partial V_{e_z}}{\partial t_s} + \frac{\partial V_{\tilde{z}_m}}{\partial t_s}\right) \\ & + d^*\mathcal{L}(f_{e_\phi,s})(V_{e_x}+V_{\tilde{x}_m}) + d^*\mathcal{L}(f_{e_\phi} - f_{e_\phi,s})(V_{e_x}+V_{\tilde{x}_m}) \\ & + d\mathcal{L}(f_{e_\phi,f})(V_{e_z}+V_{\tilde{z}_m}) + d\mathcal{L}(f_{e_\phi} - f_{e_\phi,f})(V_{e_z}+V_{\tilde{z}_m}) \end{aligned} \tag{32}$$

Conceptually this is the derivative in the subsystems plus some errors due to inaccuracies caused by the model reduction. Rearranging gives

$$\begin{aligned} \acute{V} = {} & d^*\left(\frac{\partial V_{e_x}}{\partial t_s} + \mathcal{L}(f_{e_\phi,s})V_{e_x} + \frac{\partial V_{\tilde{x}_m}}{\partial t_s} + \mathcal{L}(f_{e_\phi,s})V_{\tilde{x}_m}\right) \\ & + d^*\mathcal{L}(f_{e_\phi} - f_{e_\phi,s})V_{e_x} + d^*\mathcal{L}(f_{e_\phi} - f_{e_\phi,s})V_{\tilde{x}_m} \\ & + d\left(\frac{\partial V_{e_z}}{\partial t_s} + \mathcal{L}(f_{e_\phi,f})V_{e_z} + \frac{\partial V_{\tilde{z}_m}}{\partial t_s} + \mathcal{L}(f_{e_\phi,f})V_{\tilde{z}_m}\right) \end{aligned}$$

$$+ d\mathcal{L}(f_{e_\phi} - f_{e_\phi,f})V_{e_z} + d\mathcal{L}(f_{e_\phi} - f_{e_\phi,f})V_{\tilde{z}_m} \quad (33)$$

Some of these terms can be simplified because each Lyapunov function is not a function of all state variables (i.e. its partial derivative is zero). In doing so, ϵ must be carefully accounted for.

$$\begin{aligned}\acute{V} = d^*\left(\frac{\partial V_{e_x}}{\partial t_s} + \mathcal{L}(f_{e_\xi,s})V_{e_x} + \frac{\partial V_{\tilde{x}_m}}{\partial t_s} + \mathcal{L}(f_{\tilde{x}_m,s})V_{\tilde{x}_m}\right)\\ + d^*\mathcal{L}(f_{e_\xi} - f_{e_\xi,s})V_{e_x} + d^*\mathcal{L}(f_{\tilde{x}_m} - f_{\tilde{x}_m,s})V_{\tilde{x}_m}\\ + \frac{d}{\epsilon}\left(\frac{\partial V_{\tilde{z}_m}}{\partial t_f} + \mathcal{L}(f_{e_\eta,f})V_{e_z} + \frac{\partial V_{\tilde{z}_m}}{\partial t_f} + \mathcal{L}(f_{\tilde{z}_m,f})V_{\tilde{z}_m}\right)\\ + \frac{d}{\epsilon}\mathcal{L}(f_{e_\eta} - f_{e_\eta,f})V_{e_z} + \frac{d}{\epsilon}\mathcal{L}(f_{\tilde{z}_m} - f_{\tilde{z}_m,f})V_{\tilde{z}_m} \quad (34)\end{aligned}$$

Some of the vector fields are the same in the reduced subsystem and the full-order subsystem, which allows further simplification

$$\begin{aligned}\acute{V} = d^*\left(\frac{\partial V_{e_x}}{\partial t_s} + \mathcal{L}(f_{e_\xi,s})V_{e_x} + \frac{\partial V_{\tilde{x}_m}}{\partial t_s} + \mathcal{L}(f_{\tilde{x}_m})V_{\tilde{x}_m}\right)\\ + d^*\mathcal{L}(f_x - f_{x,s})V_{e_x}\\ + \frac{d}{\epsilon}\left(\frac{\partial V_{\tilde{z}_m}}{\partial t_f} + \mathcal{L}(f_{e_\eta,f})V_{e_z} + \frac{\partial V_{\tilde{z}_m}}{\partial t_f} + \mathcal{L}(f_{\tilde{z}_m,f})V_{\tilde{z}_m}\right)\\ + \frac{d}{\epsilon}\mathcal{L}(f_z - f_{z,f})V_{e_z} - d\mathcal{L}(f_{z_s})V_{\tilde{z}_m} \quad (35)\end{aligned}$$

Substituting the conditions from (27) and (28) gives:

$$\begin{aligned}\acute{V} \le & - d^*\alpha_1|\boldsymbol{e}_x|_2^2 - d^*\alpha_2|\tilde{\boldsymbol{x}}_m|_2^2\\ & + d^*\beta|\boldsymbol{e}_x|_2|\tilde{z}|_2\\ & - \frac{d}{\epsilon}\alpha_3|\boldsymbol{e}_z|_2^2 - \frac{d}{\epsilon}\alpha_4|\tilde{\boldsymbol{z}}_m|_2^2\\ & + \frac{d}{\epsilon}\epsilon\boldsymbol{\gamma}^T\boldsymbol{v}|\boldsymbol{e}_z|_2 + d\boldsymbol{\delta}^T\boldsymbol{v}|\tilde{\boldsymbol{z}}_m|_2 \quad (36)\end{aligned}$$

The triangle inequality shows that $|\tilde{z}|_2 \le |\boldsymbol{e}_z|_2 + |\tilde{\boldsymbol{z}}_m|_2$. Using this and rearranging gives

$$\acute{V} \le -\boldsymbol{v}^T K \boldsymbol{v} \quad (37)$$

Thus, by Lyapunov's direct method $\boldsymbol{e}_\phi \in L_\infty$. The goal is now to show that the conditions of Barbalat's Lemma are satisfied. This is done by showing that $\boldsymbol{e}_x, \boldsymbol{e}_z, \acute{\boldsymbol{e}}_x, \acute{\boldsymbol{e}}_z \in L_\infty$ and $\boldsymbol{e}_x, \boldsymbol{e}_z \in L_2$. By the arguments in Table 1 it can be concluded that these conditions are met. Note that the order of the lines in this table is significant. Thus, via Barbalat's Lemma, it is known that $\boldsymbol{e}_x, \boldsymbol{e}_z \to 0$ as $t \to \infty$. ■

Corollary 1: Let the plant exist such that the reduced slow subsystem does not require adaptive control (i.e. $\tilde{\boldsymbol{x}}_m = 0$ and $\acute{\tilde{\boldsymbol{\theta}}}_x = 0$). Assume that conditions (28b), (28c), and (28d) of Theorem 1 are true. Let the matrix $K = K^T$ be defined as

$$K \triangleq \begin{bmatrix} d^*\alpha_1 & -\frac{1}{2}(d^*\beta + d\gamma_1) & -\frac{1}{2}(d^*\beta + d\delta_1)\\ & \frac{d}{\epsilon}\alpha_3 - d\gamma_3 & -\frac{1}{2}(d\delta_3 + d\gamma_4)\\ \text{Symmetric} & & \frac{d}{\epsilon}\alpha_4 - d\delta_4 \end{bmatrix} \quad (38)$$

TABLE 1. Proof that the conditions of Barbalat's Lemma are met.

CONDITION	ARGUMENT
$\boldsymbol{e}_\phi, \acute{V} \in L_\infty$	Lyapunov's Direct Method
$\acute{\boldsymbol{e}}_\phi \in L_\infty$	Assumption 5
$\exists\lambda \in \mathbb{R}_+$ s.t. $\acute{V} \le -\lambda\lvert\boldsymbol{v}\rvert_2^2$	K is positive definite
$\lvert\boldsymbol{e}_x\rvert_2, \lvert\tilde{\boldsymbol{x}}_m\rvert_2, \lvert\boldsymbol{e}_z\rvert_2, \lvert\tilde{\boldsymbol{z}}_m\rvert_2 \in L_2$	[36, Lemma 1]
$\lvert\boldsymbol{e}_x\rvert_2, \lvert\tilde{\boldsymbol{x}}_m\rvert_2, \lvert\boldsymbol{e}_z\rvert_2, \lvert\tilde{\boldsymbol{z}}_m\rvert_2 \in L_1$	[36, Lemma 2]
$\boldsymbol{e}_x, \boldsymbol{x}_m, \boldsymbol{e}_z, \tilde{\boldsymbol{z}}_m \in L_2$	[36, Lemma 2]
$\boldsymbol{e}_x, \boldsymbol{x}_m, \boldsymbol{e}_z, \tilde{\boldsymbol{z}}_m \to 0$ as $t \to \infty$	Barbalat's Lemma

If $\exists d \in (0, 1)$ and $d^* \triangleq (1 - d)$ such that K is positive definite, then $\boldsymbol{e}_x, \boldsymbol{e}_z \to 0$ as $t \to \infty$.

Proof: The proof proceeds exactly as Theorem 1 except that $V_{\tilde{x}_m} = 0$. Also, because $\tilde{\boldsymbol{x}}_m = 0$ it follows that $\gamma_2 = 0$ and $\delta_2 = 0$. ■

Each of the following proofs assumes that $f_z - f_{z,f} = 0$ which occurs when ϵ does not appear on the right side of equation (1b). This is very common and making this assumption will aid in interpreting the results.

3) CASE 2

The fast reference model is always on the manifold.

Corollary 2: Let the plant exist such that the reduced fast subsystem does not require adaptive control ($\tilde{z}_m = 0$ and $\acute{\tilde{\boldsymbol{\theta}}}_z = 0$) and ϵ does not appear on the right side of (1b). Assume that condition (28b) of Theorem 1 is true. Then $\forall\epsilon$ it is true that $\boldsymbol{e}_x, \boldsymbol{e}_z \to 0$ as $t \to \infty$.

Proof: The proof proceeds exactly as Theorem 1 except for $\boldsymbol{\gamma} = 0$ and $\tilde{z}_m = 0$. This reduces the matrix $K = K^T$ to

$$K \triangleq \begin{bmatrix} d^*\alpha_1 & -\frac{1}{2}d^*\beta\\ -\frac{1}{2}d^*\beta & \frac{d}{\epsilon}\alpha_3 \end{bmatrix} \quad (39)$$

where $V_{\tilde{x}_m}$ has been dropped because all of the cross terms of $\tilde{\boldsymbol{x}}_m$ have been removed. This is simple enough for additional conclusions. By Sylvester's Criterion K is positive definite if and only if the leading principle minors (LPM) are positive [37]. This gives rise to the following two inequalities which, if satisfied, imply that K is positive definite.

$$0 < d^*\alpha_1 \quad (40a)$$

$$0 < \frac{d(1-d)\alpha_1\alpha_3}{\epsilon} - \frac{1}{4}(1-d)^2\beta^2 \quad (40b)$$

Inequality (40a) is satisfied by definition. Rearranging inequality (40b) gives

$$\epsilon < \frac{4d\alpha_1\alpha_3}{(1-d)\beta^2} \quad (41)$$

when $\beta \neq 0$. When $\beta = 0$ then inequality (40b) is satisfied by definition. Recall that d is arbitrary so $\forall\epsilon\ \exists d$ such that inequality (41) is satisfied. Continuing with Barbalet's Lemma as in Theorem 1 gives that $\boldsymbol{e}_x, \boldsymbol{e}_z \to 0$ as $t \to \infty$. ■

4) CASE 3

The manifold is an asymptotically stable equilibrium of the fast state reference model in the context of the full-order system.

Corollary 3: Assume that ϵ does not appear on the right-hand side of (1b). Assume that condition (28b) of Theorem 1 is true. If $\exists \alpha_4 \in \mathbb{R}_+$ such that

$$\mathcal{L}(f_{\tilde{z}_m})V_{\tilde{z}_m} \leq -\alpha_4 |\tilde{z}_m|_2^2 \tag{42}$$

then $\forall \epsilon$ it is true that $\boldsymbol{e}_x, \boldsymbol{e}_z \to 0$ as $t \to \infty$.

Proof: The proof largely follows Theorem 1 except for $V_{\tilde{x}_m}$ is removed from the composite Lyapunov function. Before reaching (35), (34) can be rewritten using $\mathcal{L}(f_{\tilde{z}_m} - f_{\tilde{z}_m,f})V_{\tilde{z}_m} + \mathcal{L}(f_{\tilde{z}_m,f})V_{\tilde{z}_m} = \mathcal{L}(f_{\tilde{z}_m})V_{\tilde{z}_m}$. Continuing to follow the proof of Theorem 1 gives

$$K \triangleq \begin{bmatrix} d^*\alpha_1 & -\frac{1}{2}d^*\beta & -\frac{1}{2}d^*\beta \\ -\frac{1}{2}d^*\beta & \frac{d}{\epsilon}\alpha_3 & 0 \\ -\frac{1}{2}d^*\beta & 0 & \frac{d}{\epsilon}\alpha_4 \end{bmatrix} \tag{43}$$

This is simple enough for additional conclusions. By Sylvester's Criterion K is positive definite if and only if the LPMs are positive. This gives rise to the following three inequalities which, if satisfied, imply that K is positive definite.

$$0 < d^*\alpha_1 \tag{44a}$$

$$0 < \frac{d(1-d)\alpha_1\alpha_3}{\epsilon} - \frac{1}{4}(1-d)^2\beta^2 \tag{44b}$$

$$0 < \frac{d^2(1-d)}{\epsilon^2}\alpha_1\alpha_3\alpha_4 - \frac{d(1-d)^2}{4\epsilon}(\alpha_3+\alpha_4)\beta^2 \tag{44c}$$

Inequality (44a) is satisfied by definition. Rearranging the other two inequalities gives

$$\epsilon < \frac{4d\alpha_1\alpha_3}{(1-d)\beta^2} \tag{45a}$$

$$\epsilon < \frac{4d\alpha_1\alpha_3\alpha_4}{(1-d)(\alpha_3+\alpha_4)\beta^2} \tag{45b}$$

when $\beta \neq 0$. When $\beta = 0$ then inequalities (44b) and (44c) are satisfied by definition. Recall that d is arbitrary and $\forall \epsilon\ \exists d$ such that the inequalities in (45) are satisfied. Continuing with Barbalet's Lemma as in Theorem 1 gives that $\boldsymbol{e}_x, \boldsymbol{e}_z \to 0$ as $t \to \infty$. ■

Remark 4: Assumption 2 places bounds on the acceptable range of the adaptation gains. Note that ϵ is not required to implement the control. This is advantageous because ϵ can be difficult to determine. However, a rough approximation of ϵ allows the engineer to design the adaptive laws and reference models so that they evolve on the correct timescale. Beyond these conditions, ϵ is allowed to be uncertain.

Remark 5: The condition that K be positive definite limits the range of acceptable timescale separation parameters (e.g. see [29]). However, for Theorem 1 and Corollary 1 the analytical bounds would be complex.

Remark 6: Corollaries 1 and 2 study the case where only one subsystem requires adaptive control. If neither subsystem requires adaptive control then Theorem 1 reduces to [35, Theorem 1].

Remark 7: Systems which use adaptive control are likely to be nonstandard because adaptive control is specifically designed for systems with model uncertainties. Thus it is common for the open-loop manifold to be uncertain even if the system is standard in the traditional sense. Let the term *uncertain nonstandard* refer to this condition. Recent multiple-timescale control research has addressed nonstandard systems [17]. Both Sequential Control and Simultaneous Slow and Fast Tracking are nonstandard methods because the manifold is specified. By comparison, Composite Control requires the open-loop manifold to be known apriori, so the manifold must be measured or analytically available. Thus Composite Control is well suited for systems that do not require adaptive control in the fast subsystem.

5) SUMMARY OF THEOREMS

This section describes each of the theorems that are proven in this article and provides criteria that can be used to determine which of the theorems apply to a given system. Theorem 1 is the most general but also has the most restrictive conditions on stability. It requires that the slow reference model be asymptotically stable to the reference model input. In practice, this can often limit the theorem to regulation. Three special cases of Theorem 1 were studied that are less restrictive. Corollary 1 is applicable when adaptive control is only used for the fast subsystem. Corollary 2 is applicable when adaptive control is only used for the slow subsystem. Corollary 3 allows adaptive control in both subsystems, but the manifold must be an asymptotically stable equilibrium of the fast reference model in the context of the full-order system.

Theorem 1 and Corollary 1 both allow the timescale separation parameter to appear on the right side of the fast states' differential equations and require checking the positive definiteness of a matrix. Corollaries 2 and 3 do not. KAMS typically requires differentiation of the manifold. In Theorem 1 and Corollary 1 the derivative of the manifold is used to ensure that condition (28d) is satisfied. The derivative of the manifold is not explicitly required for Corollary 3, but it is often required to ensure the manifold is an asymptotically stable equilibrium of the fast reference model. It is therefore significant that Corollary 2 does not require differentiating the manifold.

IV. VALIDATION

An example demonstrates and validates this method. Consider the following nonlinear, nonstandard, uncertain dynamical system

$$\acute{x} = -(x^2+1)z \tag{46a}$$

$$\epsilon\acute{z} = \theta x z + u \tag{46b}$$

where $\theta \in \mathbb{R}_+$ is an uncertain parameter. The control objective is for x to track the reference model

$$\acute{x}_m = -a_x(x_m - r_x) \tag{47}$$

where $a_x \in \mathbb{R}_+$.

A. CONTROL SYNTHESIS

The reduced slow subsystem is

$$\acute{x} = -(x^2 + 1)z_s \tag{48a}$$

and the reduced fast subsystem is

$$\grave{x} = 0 \tag{49a}$$

$$\grave{z} = \theta xz + u \tag{49b}$$

This system is uncertain and nonstandard. Sequential Control is used to fuse the control signals [17]. The slow subsystem is deterministic. Using z_s as the input to the slow subsystem the manifold is chosen using Nonlinear Dynamic Inversion (NDI).

$$z_s = -(x^2 + 1)^{-1}(\acute{x}_m - k_x e_x) \tag{50}$$

where $k_x \in \mathbb{R}_+$ is a constant control gain. The closed-loop dynamics of the reduced slow subsystem are

$$\acute{x} = \acute{x}_m - k_x e_x \tag{51}$$

or equivalently

$$\acute{e}_x = -k_x e_x \tag{52}$$

The input can now be chosen so that it drives the fast states to this manifold. The fast subsystem is parametrically uncertain. ANDI is chosen to stabilize the fast subsystem

$$u = \grave{z}_m - \hat{\theta} xz - k_z e_z \tag{53}$$

where $k_z \in \mathbb{R}_+$ is a constant control gain. The adaptive law for $\hat{\theta}$ is

$$\grave{\hat{\theta}} = \gamma \ \mathrm{Proj}(\hat{\theta}, xze_z) \tag{54}$$

where $\gamma \in \mathbb{R}_+$ is an adaptation rate gain. For more information on ANDI see [27, p. 6–12]. The fast state reference model is chosen to be asymptotically stable about the manifold

$$\grave{\tilde{z}}_m = -a_z \tilde{z}_m \tag{55}$$

or equivalently

$$\grave{z}_m = -a_z \tilde{z}_m + \grave{z}_s \tag{56}$$

where $a_z \in \mathbb{R}_+$. The time derivative of the manifold is

$$\begin{aligned} \grave{z}_s = {} & \frac{2xz\epsilon}{x^2+1}(a_x \tilde{x}_m + k_x e_x) \\ & + \frac{\epsilon}{x^2+1}(-a_x(a_x \tilde{x}_m + \acute{r}_x) \\ & + k_x(-(x^2+1)z + a_x \tilde{x}_m)) \end{aligned} \tag{57}$$

B. CONFIRMATION OF FULL-ORDER STABILITY

Consider the candidate Lyapunov functions

$$V_{e_x} = \frac{1}{2} e_x^2 \tag{58a}$$

$$V_{e_z} = \frac{1}{2} e_z^2 + \frac{1}{2\gamma} \tilde{\theta}^2 \tag{58b}$$

$$V_{\tilde{z}_m} = \frac{1}{2} \tilde{z}_m^2 \tag{58c}$$

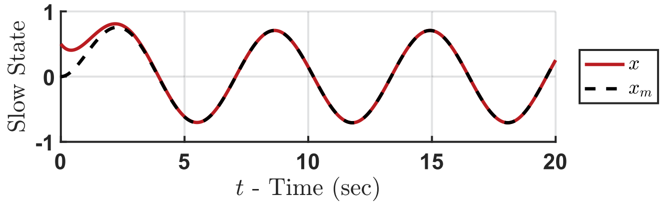

FIGURE 4. Evolution of the slow state.

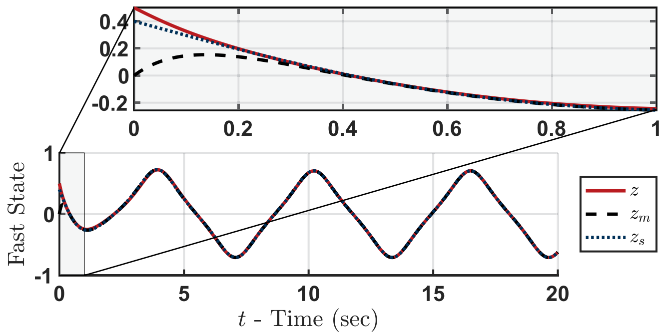

FIGURE 5. Evolution of the fast state.

Differentiating gives

$$\mathcal{L}(f_{e_\xi,s})V_{e_x} = -k_x e_x^2 \qquad \le -\alpha_1 |e_x|_2^2 \tag{59a}$$

$$\mathcal{L}(f_{e_\eta,f})V_{e_z} \le -k_z e_z^2 \qquad \le -\alpha_3 |e_z|_2^2 \tag{59b}$$

$$\mathcal{L}(f_{\tilde{z}_m})V_{\tilde{z}_m} = -a_z \tilde{z}_m \qquad \le -\alpha_4 |\tilde{z}_m|_2^2 \tag{59c}$$

$$\mathcal{L}(f_x - f_{x,s})V_{e_x} = -(x^2+1)e_x \tilde{z} \qquad \le \beta |e_x|_2 |\tilde{z}|_2 \tag{59d}$$

where $\alpha_1 = k_x$, $\alpha_3 = k_z$, $\alpha_4 = a_z$, and $\beta = 1$. See [27, Equations 1.20 to 1.23] for a derivation of (59b). By Corollary 3, $\boldsymbol{e}_x, \boldsymbol{e}_z \to 0$ as $t \to \infty$.

C. NUMERICAL RESULTS

A numerical simulation validates the control. The system parameters are

$$\theta = 0.5 \tag{60a}$$

$$\epsilon = 0.1 \tag{60b}$$

and the control parameters are

$$r_x = \sin(t_s) \tag{61a}$$

$$a_x = k_x = a_z = k_z = \gamma = 1 \tag{61b}$$

with initial conditions

$$x = z = 0.5 \tag{62a}$$

$$x_m = z_m = 0 \tag{62b}$$

$$\hat{\theta} = 0.44 \tag{62c}$$

The time evolution of the slow state is shown in Fig. 4 and the fast state is shown in Fig. 5. The time evolution of the adapting gain is shown in Fig. 6. The states and gain evolve on the proper timescales and the system converges asymptotically with zero steady-state error.

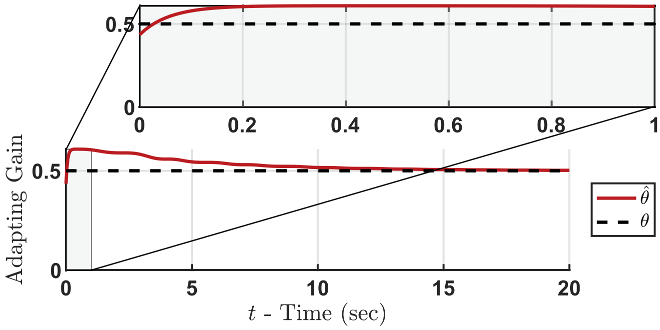

FIGURE 6. Evolution of the adapting gain.

D. ALTERNATIVE APPROACH

Corollary 1 is also applicable because adaptive control is only required for the fast subsystem. To demonstrate this the problem is revised to a regulation problem and the fast reference model is redefined so that it is no longer *asymptotically* stable about the manifold

$$\grave{\tilde{z}}_m = -a_z \tilde{z}_m \tag{63}$$

Note that the manifold is still a stable equilibrium. It is even asymptotically stable when the manifold is constant with respect to time, but it is not *asymptotically* stable in the context of the full-order system. Reference models such as this are useful if $\acute{\boldsymbol{r}}_x$ is not known apriori or the manifold is difficult to differentiate. From (57) it can be shown that

$$-\mathcal{L}(f_{z_s})V_{\tilde{z}_m} = \left(-\frac{2xz}{x^2+1}k_x e_x + k_x z\right)\tilde{z}_m \tag{64a}$$

$$\leq \left(2k_x|e_x|_2 + k_x|z|_2\right)|\tilde{z}_m|_2 \tag{64b}$$

$$\leq \begin{bmatrix} 2k_x + k_x^2 & 0 & k_x & k_x \end{bmatrix} \boldsymbol{v}|\tilde{z}_m|_2 \tag{64c}$$

$$\leq \boldsymbol{\delta}^T \boldsymbol{v}|\tilde{z}_m|_2 \tag{64d}$$

where the domain has been restricted to $x < 1$ and $z < 1$. Note that $\delta_1 = 2k_x + k_x^2$, $\delta_2 = 0$, $\delta_3 = k_x$, and $\delta_4 = k_x$. Substituting the values from the previous numerical example gives

$$K \triangleq \begin{bmatrix} d^* & -\frac{1}{2}d^* & -\frac{1}{2}(d^* + 3\,d) \\ -\frac{1}{2}d^* & \frac{d}{\epsilon} & -\frac{1}{2}d \\ -\frac{1}{2}(d^* + 3\,d) & -\frac{1}{2}d & \frac{d}{\epsilon} - d \end{bmatrix} \tag{65}$$

From Corollary 1 it is known that if $\exists d \in (0, 1)$ and $d^* \triangleq (1 - d)$ such that K is positive definite then $\boldsymbol{e}_x, \boldsymbol{e}_z \to 0$ as $t \to \infty$. By Sylvester's Criterion K is positive definite if and only if the LPMs are positive. The first LPM is positive by definition. The second and third LPMs depend upon ϵ and d. Fig. 7 plots this relationship. If both LPMs are positive for a given ϵ then the conditions of Corollary 1 are satisfied. In Fig. 7 note that as ϵ increases there is a point after which $\nexists d$ such that both LPMs are positive simultaneously. At this point, the timescale separation is insufficient for Corollary 1 to guarantee convergence.

From Fig. 7 it can also be seen that when $\epsilon = 0.1$ (as in the previous example) $\exists d$ such that all of the LPMs are positive. Thus by Corollary 1 $\boldsymbol{e}_x, \boldsymbol{e}_z \to 0$ as $t \to \infty$. The time evolution of the slow state for this alternative approach is shown in Fig. 8; the fast state is shown in Fig. 9; and the time evolution of the adapting gain is shown in Fig. 10. This example demonstrates how the manifold evolves on the slow timescale per Assumption 3.

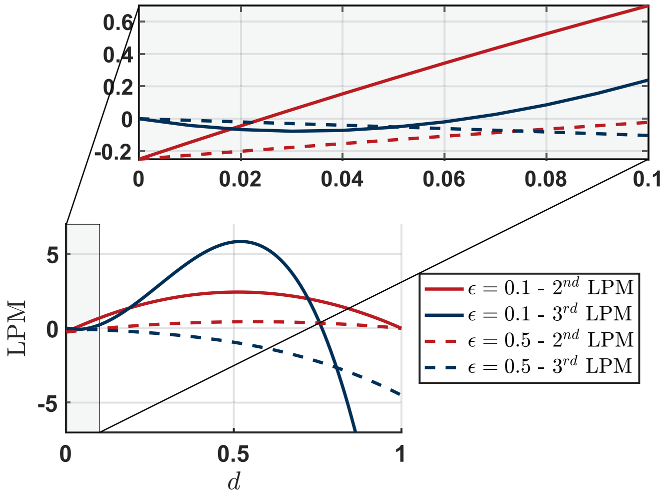

FIGURE 7. Effects of varying ϵ and d on the applicablility of Corollary 1.

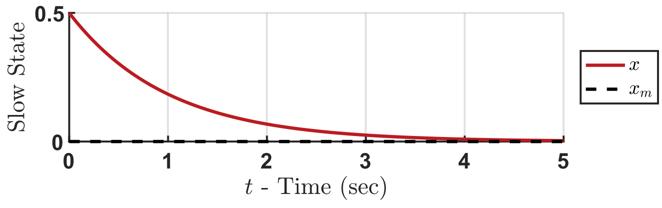

FIGURE 8. Evolution of the slow state for the alternative approach.

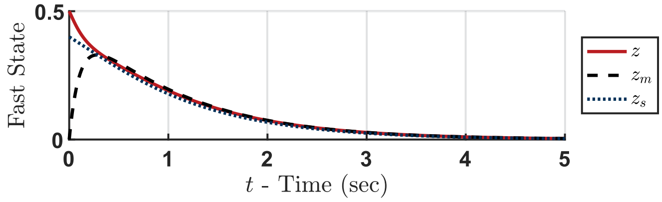

FIGURE 9. Evolution of the fast state for the alternative approach.

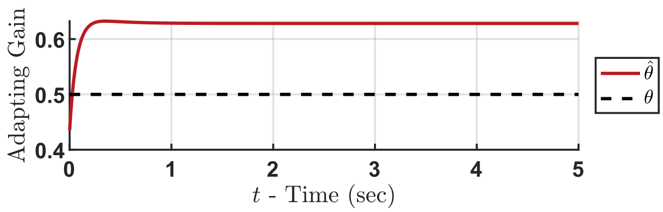

FIGURE 10. Evolution of the adapting gain for the alternative approach.

Remark 8: As mentioned previously a common approach to these problems is to apply sequential loop closure to the subsystems. This example uses Sequential Control. To clarify Sequential Control is an extension of sequential loop closure. Applying sequential loop closure to this example would yield numerically indistinguishable results. Sequential Control was first published by Narang-Siddarth and Valasek in [17] where they showed that singular perturbation techniques could be used to rigorously show stability and obtain specific bounds on the time scale separation parameter. By extension, this same advantage is available to KAMS. The insights from Fig. 7 are a unique contribution of KAMS that is not available to traditional adaptive sequential loop closure implementations. Furthermore, unlike sequential loop closure, KAMS allows the use of Composite Control and Simultaneous Slow and Fast Tracking.

Remark 9: The MATLAB code used for both of the examples has been made open source and is available on Code Ocean [38].

V. CONCLUSION

This article extended the [K]control of Adaptive Multiple-timescale Systems (KAMS) methodology to singularly perturbed systems with adaptive control in both the fast and slow subsystems; a wide class of adaptive control and multiple-timescale control methods fit within this framework. Sufficient conditions for asymptotic stability were proven and coupling effects between the manifold and the fast reference model were identified. The stability of the full-order system was connected to the stability of the reduced-order systems through Theorem 1 and its corollaries. A nonlinear nonstandard system was used to demonstrate KAMS.

This article identified complex interactions between the fast reference model and the manifold which occur when adaptive control is used to stabilize the fast subsystem. This makes traditional multiple-timescale control proofs insufficient when adaptive control is used in the fast subsystem. The theorems proved in this article account for these complex interactions by carefully formatting the augmented error dynamics and by judiciously selecting sufficient conditions. The primary limitation of KAMS is the requirement to verify the conditions given in Theorem 1 and its corollaries. These conditions restrict the set of systems to which the theorems in this article can be applied. Lyapunov functions may not be known for some systems and adaptive control methods. Suitable Lyapunov functions are known for several popular adaptive control methods (e.g. Model Reference Adaptive Control and Adaptive Nonlinear Dynamic Inversion). Another limitation is that many applications will require differentiation of the manifold. This can be a complicated calculation, but it can sometimes be avoided by judicious selection of control objectives, careful system modeling, and the use of the correct corollary. See the alternative approach example above for a demonstration of this. Based upon the results presented in the article KAMS is judged to be a feasible control approach for uncertain nonstandard singularly perturbed systems regardless of which subsystem (fast, slow, or both) the uncertainty appears in. Further, KAMS is more capable than traditional sequential loop closure because it can be used to determine the minimum allowable timescale separation and it allows for the use of Composite Control and Simultaneous Slow and Fast Tracking.

There are several potential avenues for future research. First, future research could consider adapting laws that do not adapt in the same timescale as the subsystem to which they are applied. Second, future research could determine alternate formats for the upper bounds in Theorem 1. Finally, experimentally validating the performance of KAMS on physical systems would be insightful.

ACKNOWLEDGMENT

The technical monitor is Brian Holm-Hansen. This support is gratefully acknowledged by the authors. Any opinions, findings, conclusions or recommendations expressed in this material are those of the authors and do not necessarily reflect the views of the U.S. Navy.

REFERENCES

[1] D. S. Naidu and A. J. Calise, “Singular perturbations and time scales in guidance and control of aerospace systems: A survey,” *J. Guid., Control, Dyn.*, vol. 24, no. 6, pp. 1057–1078, Dec. 2001.
[2] A. Narang-Siddarth and J. Valasek, “Global tracking control structures for nonlinear singularly perturbed aircraft systems,” in *Proc. 1st CEAS Specialist Conf. Guid., Navigation Control*, Munchen, Germany, 2011, pp. 235–246.
[3] H. M. Soner, “Singular perturbations in manufacturing,” *Soc. Ind. Appl. Math. J. Control Optim.*, vol. 31, no. 1, pp. 132–146, 1993.
[4] M. A. Al-Radhawi, M. Sadeghi, and E. D. Sontag, “Long-term regulation of prolonged epidemic outbreaks in large populations via adaptive control: A singular perturbation approach,” *Control Syst. Lett.*, vol. 6, pp. 578–583, May 2021.
[5] E. Rollins, “Nonlinear adaptive dynamic inversion control for hypersonic vehicles,” Ph.D. dissertation, Texas A&M Univ., College Station, TX, USA, Dec. 2013.
[6] D. Famularo, J. Valasek, J. A. Muse, and M. A. Bolender, “Enforcing state constraints on a model of a hypersonic vehicle,” in *Proc. AIAA Guid., Navigation, Control Conf.*, 2016, pp. 1–13.
[7] N. Hovakimyan, E. Lavretsky, and A. Sasane, “Dynamic inversion for nonaffine-in-control systems via time-scale separation. Part I,” *J. Dyn. Control Syst.*, vol. 13, no. 4, pp. 451–465, Oct. 2007.
[8] N. Hovakimyan, E. Lavretsky, and C. Cao, “Adaptive dynamic inversion via time-scale separation,” *IEEE Trans. Neural Netw.*, vol. 19, no. 10, pp. 1702–1711, Oct. 2008.
[9] S. Sastry and M. Bodson, *Adaptive Control: Stability, Convergence, and Robustness* (Prentice Hall Informationn and System Sciences Series). Englewood Cliffs, NJ, USA: Prentice Hall, 1989.
[10] A. Macchelli, D. Barchi, L. Marconi, and G. Bosi, “Robust adaptive control of a hydraulic press,” *IFAC-PapersOnLine.*, vol. 53, pp. 8790–8795, Jul. 2020.
[11] N. Nguyen, K. Krishnakumar, and J. Boskovic, “An optimal control modification to model-reference adaptive control for fast adaptation,” in *Proc. AIAA Guid., Navigation Control Conf. Exhib.*, 2008, pp. 1–20.
[12] K. Eves and J. Valasek, “Slow time scale adaptive control for multiple time scale systems,” *J. Guid., Control, Dyn.*, vol. 46:11, pp. 2063–2075, 2023.
[13] D. Saha and J. Valasek, “Two-time-scale slow and fast state tracking of an f-16 using slow and fast controls,” in *Proc. AIAA Guid., Navigation, Control Conf.*, 2017, pp. 1–17.
[14] D. Saha, J. Valasek, and M. M. Reza, “Two-time-scale control of a low-order nonlinear, nonstandard system with uncertain dynamics,” in *Proc. IEEE Annu. Amer. Control Conf.*, 2018, pp. 3720–3725.
[15] D. Saha and J. Valasek, “Nonlinear multiple-time-scale attitude control of a rigid spacecraft with uncertain inertias,” in *Proc. AIAA SciTech Forum*, 2019, pp. 1–20.

[16] D. Saha, J. Valasek, C. Leshikar, and M. M. Reza, “Multiple-timescale nonlinear control of aircraft with model uncertainties,” *J. Guid., Control, Dyn.*, vol. 43, no. 3, pp. 536–552, 2020.
[17] A. Narang-Siddarth and J. Valasek, *Nonlinear Multiple Time Scale Systems in Standard and Non-Standard Forms: Analysis & Control*, 1st ed. Philadelphia, PA, USA: SIAM, 2014.
[18] P. A. Ioannou and J. Sun, *Robust Adaptive Control*. Hoboken, NJ, USA: Prentice Hall, 1996.
[19] E. Lavretsky and K. A. Wise, *Robust and Adaptive Control with Aerospace Applications* (Advanced Textbooks in Control and Signal Processing Series). London, U.K.: Springer, 2013.
[20] N. T. Nguyen, *Model-Reference Adaptive Control A Primer* (Advanced Textbooks in Control and Signal Processing Series). Berlin, Germany: Springer, 2018.
[21] P. Kokotovic, H. K. Khalil, and J. O’Reilly, *Singular Perturbation Methods in Control Analysis and Design*, 2nd ed. Philadelphia, PA, USA: SIAM, 1999.
[22] A. H. Nayfeh, *Perturbation Methods*. New York, NY, USA: Wiley, 1973.
[23] A. Isidori, *Nonlinear Control Systems*. London, U.K.: Springer, 1995.
[24] R. Santos and T. R. Oliveira, “Trajectory tracking for uncertain (non)minimum phase systems by monitoring function and time-scaling based sliding mode control,” *IFAC J. Syst. Control*, vol. 12, 2020, Art. no. 100089.
[25] M. Picallo, S. Bolognani, and F. Dörfler, “Sensitivity conditioning: Beyond singular perturbation for control design on multiple time scales,” *IEEE Trans. Autom. Control*, vol. 68, no. 4, pp. 2309–2324, Apr. 2023.
[26] T. R. Oliveira, L. R. Costa, J. M. Y. Catunda, A. V. Pino, W. Barbosa, and M. N. d. Souza, “Time-scaling based sliding mode control for neuromuscular electrical stimulation under uncertain relative degrees,” *Med. Eng. Phys.*, vol. 44, pp. 53–62, 2017.
[27] D. Famularo, “Observer-based nonlinear dynamic inversion adaptive control with state constraints,” Ph.D. dissertation, Texas A&M Univ., College Station, TX, USA, Sep. 2017.
[28] F. L. Lewis and M. Vandegrift, “Flexible robot arm control by a feedback linearization/singular perturbation approach,” in *Proc. IEEE Int. Conf. Robot. Automat.*, 1993, pp. 729–736.
[29] A. Saberi and H. Khalil, “Quadratic-type Lyapunov functions for singularly perturbed systems,” *IEEE Trans. Autom. Control*, vol. 29, no. 6, pp. 542–550, Jun. 1984.
[30] P. D. Christofides, A. R. Teel, and P. Daoutidis, “Robust semi-global output tracking for nonlinear singularly perturbed systems,” in *Proc. IEEE Conf. Decis. Control*, 1995, pp. 2251–2256.
[31] D. Saha and J. Valasek, “Observer-based sequential control of a nonlinear two-time-scale spring-mass-damper system,” in *Proc. AIAA Guid., Navigation, Control Conf.*, 2016, Art. no. 0361.
[32] D. Saha and J. Valasek, “Observer-based sequential control of a nonlinear two-time-scale spring-mass-damper system with multiple slow and fast states,” *IFAC-PapersOnLine*, vol. 49, no. 18, pp. 684–689, 2016.
[33] J. Deese and C. Vermillion, “Real-time experimental optimization of closed-loop crosswind flight of airborne wind energy systems via recursive Gaussian process-based adaptive control,” in *Proc. IEEE Conf. Control Technol. Appl.*2020, pp. 516–521.
[34] H. K. Khalil, *Nonlinear Systems*, 3rd ed. Hoboken, NJ, USA: Prentice Hall, 2002.
[35] A. Saberi and H. Khalil, “Stabilization and regulation of nonlinear singularly perturbed systems–Composite control,” *IEEE Trans. Autom. Control*, vol. 30, no. 8, pp. 739–747, Aug. 1985.
[36] K. Eves and J. Valasek, “Adaptive control for non-minimum phase systems via time scale separation,” in *Proc. IEEE Amer. Control Conf.*, 2023, pp. 4223–4228.
[37] G. T. Gilbert, “Positive definite matrices and Sylvester’s criterion,” *Amer. Math. Monthly*, vol. 98, pp. 44–46, Jan. 1991.
[38] K. Eves and J. Valasek, “Adaptive control for singularly perturbed systems examples,” *Code Ocean*, Aug. 2023. [Online]. Available: https://codeocean.com/capsule/4989235/tree

KAMERON EVES (Member, IEEE) received the B.S. degree in mechanical engineering from Brigham Young University, Provo, UT, USA, in 2019, and the Ph.D. degree in aerospace engineering from Texas A&M University, College Station, TX, USA, in 2023. In 2023, he became an Assistant Professor of electrical and computer engineering with Utah Tech University, St. George, UT. Before that, he was a Graduate Research Assistant with Texas A&M University working with the Vehicle Systems and Control Laboratory with Dr. John Valasek. His research interests generally include theoretical dynamics and control with a focus on aerospace applications. His recent work includes nonlinear control (primarily adaptive control) and reinforcement learning for fixed-wing aircraft and uncrewed air vehicles (UAV). Dr. Eves is a member of the Control Systems Society and the Education Society.

JOHN VALASEK (Senior Member, IEEE) received the B.S. degree in aerospace engineering from California State Polytechnic University, Pomona, CA, USA, in 1986, the M.S. degree (with Hons.) and the Ph.D. degree in aerospace engineering from the University of Kansas, Lawrence, KS, USA, in 1990 and 1995, respectively. He was a Flight Control Engineer with the Flight Controls Research Group, Aircraft Division, Northrop Corporation, where he worked on the AGM-137 Tri-Services Standoff Attack Missile Program. He was also a Summer Faculty Researcher with NASA Langley in 1996 and an Air Force Office of Scientific Research Summer Faculty Research Fellow with the Air Force Research Laboratory in 1997. Since then, he has been with the Department of Aerospace Engineering, Texas A&M University, College Station, TX, USA, where he is a Thaman Professor of Undergraduate Teaching Excellence, Professor of aerospace engineering, and member of the Honors Faculty. He is the Director of the Vehicle Systems & Control Laboratory, where his research is focused on bridging the scientific gaps between traditional computer science topics and aerospace engineering topics, while achieving a high degree of closure between theory and experiment from guidance, navigation and control theory to Unmanned Air Systems (UAS) to General Aviation flight safety to smart materials. He has written four books including *Nonlinear Time Scale Systems in Standard and Nonstandard Forms* (SIAM, 2014). His research interests include nonlinear control of systems with multiple timescales, autonomous and nonlinear control of cyber-physical air, space and ground systems, machine learning and multiagent systems, and vision-based navigation systems. Dr. Valasek is a member of the Control Systems Society, Systems, Man, and Cybernetics Society, Computational Intelligence Society, and the Education Society. He was an Associate Editor for Dynamics and Control of IEEE TRANSACTIONS ON EDUCATION during 1998–2001.